

# FATIGUE FRACTURE OF POLY(METHYL METHACRYLATE) BONE CEMENT CONTAINING RADIOPACIFIER NANOPARTICLES

A. BELLARE, M.E. TURELL, A. GOMOLL and T.S. THORNHILL  
Department of Orthopaedic Surgery, Brigham & Women's Hospital, Harvard Medical School, Boston, MA, USA

## ABSTRACT

Poly(methyl methacrylate) (PMMA) based bone cement has been widely used for fixation of total joint replacement prostheses for over 40 years. Commercial bone cements is usually packaged as two components: (1) liquid MMA monomer and (2) a powder component containing prepolymerized beads of PMMA of 20-100 micrometer diameter, along with 1 micrometer diameter radiopacifier particles of barium sulfate or zirconium oxide and benzoyl peroxide reaction initiator. The 2.5 volume percent of radiopacifier particles are necessary to enable orthopaedic surgeons to monitor fatigue fracture of cement in the patient using x-ray radiographs. A major problem associated with these particles is that their incomplete dispersion leads to the presence of large defects, ultimately decreasing the fatigue properties of the cement. In this study, we replaced the 1 micrometer size barium sulfate particles present in commercial PMMA cements with an identical quantity of 35 nm size barium sulfate particles. The dispersion of barium sulfate particles in PMMA cement was characterized using low voltage scanning electron microscopy and ultra-small angle x-ray scattering performed at the UNICAT beamline of the Advanced Photon Source, Argonne National Laboratory, Argonne, IL. Uniaxial tensile tests showed that the nanocomposite cement had a substantially higher work-of-fracture compared to the cement containing the micrometer size particles. There were no significant differences in the work-of-fracture obtained from steady state crack propagation tests conducted on compact tension specimens of radiopaque cements. The fatigue life of notched dogbone shaped cement specimens was measured by subjecting them to cyclic loading. The nanocomposite cement had a substantially higher fatigue life compared to the microcomposite cement. Fracture surfaces of the cement displayed evidence of plastic deformation in the regions surrounding the nanoparticle fillers. Plastic deformation of PMMA preceding crack propagation is the most plausible mechanism underlying the high fatigue fracture resistance of bone cements containing nanoparticles fillers.

## 1 INTRODUCTION

Polymethyl methacrylate (PMMA) based bone cement has been used for nearly four decades for fixation of total joint replacement prostheses. Several factors are important for this clinical application, such as setting times of the cement, volumetric shrinkage and fatigue life. Among these factors, the fatigue life of cement has received the most attention since cement fracture in patients can lead to implant loosening, resulting in early revision surgery. It is now also well known that dispersion of radiopacifiers, usually 10 weight percent of approximately 1  $\mu\text{m}$  size barium sulfate or zirconium oxide particles, has been associated with cement fracture, as shown by Topoleski [1], de Wijn [2] and Beaumont [3], and reviewed by Demian [4]. In this study, we studied the effect of barium sulfate dispersion on the mechanical properties of CMW1 bone cement (Johnson & Johnson/Depuy Orthopedics Inc) using three different mechanical tests: uniaxial tensile, high rate fracture toughness and crack propagation tests in the fatigue mode. We hypothesized that a reduction in barium sulfate particle size from 1  $\mu\text{m}$  to 100nm, along with improved dispersion would result in an increase in the mechanical properties of the resulting "nanocomposite" cement. The results showed that while the work-of-fracture of the nanocomposite increased in tensile tests, there was a decrease in the work-of-fracture in high rate,

crack propagation tests. However, in contrast to the rapid, constant speed, crack propagation tests, there was a substantial increase in the fatigue life of the nanocomposite cement in crack propagation tests under cyclic loads, drawing attention to the importance of the mechanism of crack propagation and their clinical relevance.

## 2 MATERIALS AND METHODS

All tests were performed on CMW1 bone cement (Johnson&Johnson/Depuy, Warsaw, IN) since the powder component of these cements does not contain pre-mixed barium sulfate powder. The 1  $\mu$ m barium sulfate powder contained in CMW1 cement packages and 100 nm size (nanosized) powder (Sachtleben, Duisburg, Germany) were mixed into separate batches of CMW1 cements in the standard quantity of 10 weight %, which, upon setting using a standard vacuum mixing method, resulted in "microcomposite" (conventional CMW1 cement) and "nanocomposite" cements, respectively. Radiolucent (unfilled) CMW1 was used as a control to study the effect of the presence of barium sulfate and their size and dispersion. ASTM standard tensile tests and compact tension fracture toughness tests were performed at room temperature using an Instron 4201 tensile tester. Crosshead speeds of 1mm/sec and 50mm/sec, respectively, were used for the two short-term tests. Long term, fatigue tests were performed on an Instron 8511 servo-hydraulic testing machine. Prior to testing, the specimens were soaked in room temperature water for 2 days. During testing, the specimens were maintained at 37C using a recirculating water bath. The pre-notched specimens were fatigued in load control with an R-ratio (minimum load to maximum load) of 0.03 and stress amplitude of 15 MPa at a frequency of 2 Hz. Specimens that failed at the grips were discarded. Sample size ranged from 6-10. A JEOL 6320FV low voltage scanning electron microscope (LVSEM) was used to examine the fracture surfaces of fatigue specimens. In addition, ultra-small angle x-ray scattering (USAXS) at the UNICAT synchrotron x-ray beamline of the Advanced Photon Source, Argonne National Laboratory, Argonne, IL was used to quantify the dispersion of radiopacifier particles in the microcomposite and nanocomposite PMMA cements. Sheets of 0.5mm thickness of each type of cement were subjected to USAXS using 10 keV x-rays and a beam cross-sectional area of 2mm x 0.6mm. The x-ray scattering curves were analyzed using Porod's law to characterize the surface area to volume ratio (specific surface area) of dispersed radiopacifier particles as well as voids within the PMMA matrix.

## 3 RESULTS

The work-of-fracture (WOF) was calculated for the short-term mechanical tests: the uniaxial tensile and compact tension fracture toughness tests (see Table 1). The load-displacement curve of the compact tension tests displayed unstable crack propagation behavior characteristic of brittle materials, indicating that all three samples exhibited brittle behavior.

Table 1: Tensile work of fracture (WOF) and Compact tension work of fracture (CTS WOF) for radiolucent (unfilled), microcomposite and nanocomposite bone cements.

Sample Type	Tensile WOF [MJ/m <sup>3</sup> ]	CTS WOF [N/m <sup>2</sup> ]
Radiolucent	2.77 $\pm$ .64	564.22 $\pm$ 138.02
Microcomposite	1.73 $\pm$ .46	566.28 $\pm$ 106.13
Nanocomposite	2.94 $\pm$ .67	476.26 $\pm$ 100.30

The tensile test results showed that the presence of 1  $\mu$ m size barium sulfate decreased the tensile WOF by 38% (p<0.05; ANOVA) but there was no statistically significant difference between the tensile WOF of radiolucent and the nanocomposite cements. In contrast, a comparison of the compact tension WOFs showed no statistically significant difference between the microcomposite and radiolucent cement while the WOF of the nanocomposite decreased by 16% (p<0.05;

ANOVA) compared to the radiolucent cement. For the fatigue tests, the number of cycles to failure (or total fatigue life) was recorded, as shown in Figure 1.

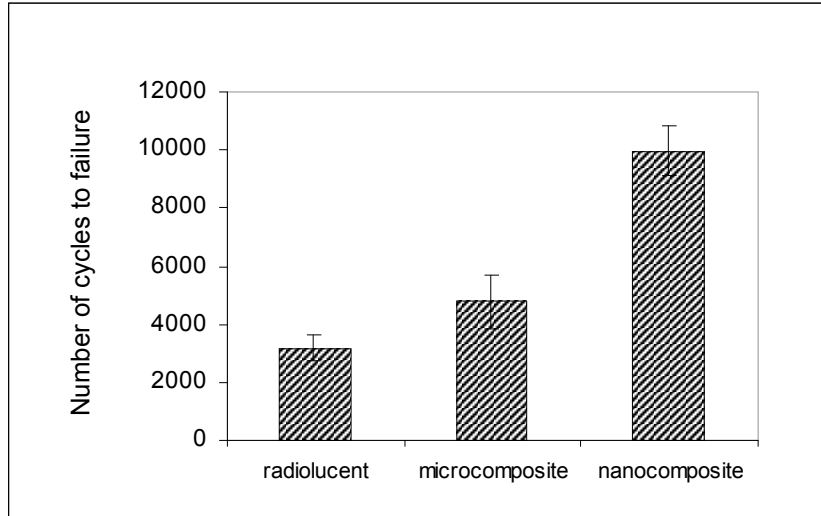


Figure 1: Total Fatigue Life of Cements

The number of cycles to failure increased by 50% for the microcomposite, and by over 200% in the nanocomposite cements, compared to the radiolucent CMW1 cement. A comparison of the fracture surfaces of the compact tension and fatigue specimens showed that the crack propagated through most of the PMMA prepolymerized beads in the path of the rapidly propagating crack in the compact tension tests, while the crack propagation occurred through more of the inter-bead matrix region in the fatigue tests. Figure 2 shows fracture surfaces of compact tension specimens of the microcomposite and nanocomposite cement, which display the well-dispersed microparticles and nanoparticles of barium sulfate.

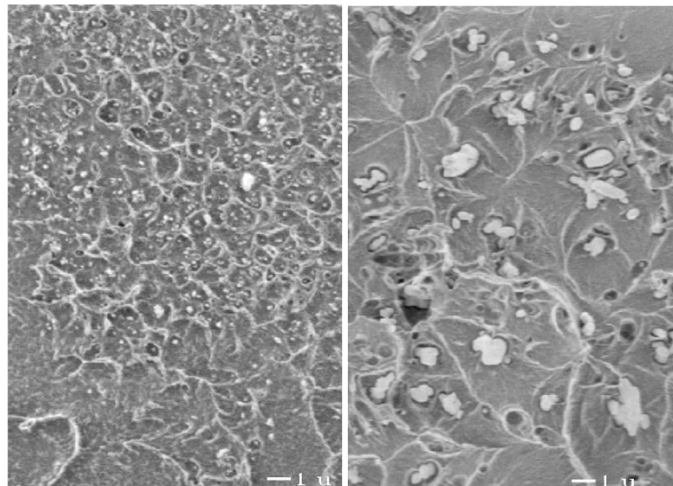


Figure 2: LVSEM fractographs of nanocomposite (left) and microcomposite (right) cements.

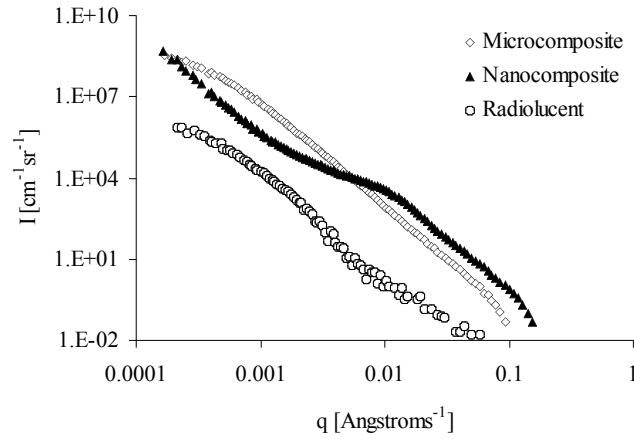


Figure 3: USAXS scattering functions (I) versus scattering vector, (q) for various cements

USAXS scattering curves were obtained by plotting the scattered intensity (I) versus (q) as shown in Figure 3, where the scattering vector, q, is defined by eqn (1):

$$q = \frac{4\pi}{\lambda} \sin \theta \quad (1)$$

where  $\theta$  equals one half of the scattering angle and  $\lambda$  is the wavelength of x-rays ( $\lambda = 2.38$  Angstrom). USAXS revealed a substantial scattering intensity due to the presence of both voids (radiolucent cement) as well as due to barium sulfate particles. The region of the scattering curve at  $q > 0.008$  [Angstrom<sup>-1</sup>] was curve fitted to a Power law function which is shown in eqn (2) and eqn (3):

$$I(q) = Kq^{-4} \quad (2)$$

$$\text{where } K = 2\pi^2 \Delta\rho^2 (S/V) \quad (3)$$

such that  $\Delta\rho$  is the electron density difference between barium sulfate (or voids, in the case of radiolucent cement) and PMMA and (S/V) is the specific surface area of the scattering entity (radiopacifier or voids). The scattering invariant, Q, was calculated for all cement samples using the area under the scattering curve,  $q^2 I(q)$  versus q. The invariant for an angular range of  $0 - q_{\min}$  was calculated by fitting the low q region of the scattering curve using Guinier's Law, and Porod's law was used for  $q_{\max} -$ . The specific surface area can then be defined by eqn (4):

$$S/V = \pi (K/Q) \quad (4)$$

Porod analysis showed that the ratio of the specific surface area for the nanocomposite and microcomposite cements respectively was 9.16 (Table 2).

Table 2: Specific surface area obtained using USAXS for various bone cements

Sample	Specific Surface Area (S) [cm <sup>-1</sup> ]
Radiolucent	$6.16147 \times 10^5$
Microcomposite	$2.39404 \times 10^5$
Nanocomposite	$2.19348 \times 10^6$

#### 4 DISCUSSION

This study shows that the presence of barium sulfate, the particle size, and their dispersion strongly affect their mechanical properties. In addition, it also shows that constant speed, rapid crack propagation and the long term, cyclic load (fatigue) crack propagation tests probe different mechanisms of crack propagation, as demonstrated previously by Topoleski [5] using conventional bone cements. In the case of the fatigue tests employed in this study, the presence of barium sulfate had a much larger effect on the overall properties since the slow crack propagated through the weaker inter-bead matrix region of PMMA. In contrast, the differences in compact tension WOF were small since the crack propagated through the PMMA beads, which usually comprise 2/3<sup>rd</sup> of the overall volume of cement, thereby decreasing the influence of the barium sulfate on the macroscopic properties. Thus, LVSEM was important in revealing the mechanism of crack growth in these two fracture toughness experiments.

The use of barium sulfate nanoparticles led to a substantial increase in the fatigue life of CMW1 at the chosen test conditions. All samples were pre-notched prior to cyclic loading thereby testing the resistance of the cements to crack propagation. It must be noted that the samples were screened using x-ray radiographs for the presence of large bubbles. All samples with visible bubbles in the anticipated path of crack propagation were discarded so that the results would reflect the toughening of cement due to radiopacifier size and dispersion alone. We also plan to perform tests for resistance to crack initiation for these new nanocomposite cements. If crack initiation is flaw driven, and if the major source of flaws is the agglomeration of radiopacifiers, we believe that the nanocomposite may have improved resistance to crack initiation as well.

This study also showed that USAXS is effective in quantitatively measuring the specific surface area of barium sulfate radiopacifiers dispersed within PMMA bone cement. It is expected that for the same volume (or weight) fraction, the nanometer size particles must have a total specific surface area that is 10 times larger than the micrometer size particles in bone cement since there would be a 1000 times more particles of 1/10<sup>th</sup> of the diameter. The value of 9.16 is in excellent agreement with this calculation, considering that the inherent particle size distributions can alter the ratio of specific surface area. Agglomeration of particles would result in a reduction in specific surface area. USAXS therefore showed that both microcomposite and nanocomposite cement had relatively well-dispersed radiopacifier particles. In addition, USAXS was able to provide the specific surface area of voids. This technique could be used to guide in the development of new mixing protocols with the objective of reducing voids since these flaws can also reduce the fracture toughness of cements. LVSEM confirmed the quantitative analysis provided by USAXS measurements by revealing fracture surfaces where particles were uniformly dispersed throughout the PMMA matrix. The most interesting observation was on the fracture surfaces of the 100nm size BaSO<sub>4</sub> containing cement. The inter-bead matrix region containing the BaSO<sub>4</sub> nanoparticles showed a very high concentration of approximately, 1-2  $\mu$ m diameter fracture "craters" with a rim comprising "tufts" of plastically deformed PMMA. This indicates that the PMMA surrounding the particles were subjected to plastic strain prior to crack propagation. This is in agreement with our tensile tests, which showed a higher WOF in the "nanocomposite" cement. Thus, the dispersed BaSO<sub>4</sub> nanoparticles set up the PMMA matrix to plastically deform (although only to a small extent) during crack propagation, thereby exhibiting a "nanotoughening" effect. While these differences in WOF and amount of plastic deformation are not large compared to rubber-toughened PMMA, they have broad implications for fatigue crack propagation rates, which is a concern for the application of bone cements in orthopaedic implants. In conclusion, the fatigue performance of acrylic cements can be substantially improved by a uniform dispersion of barium sulfate nanoparticles. These must however be more rigorously tested under conditions that simulate their in vivo loading and biological environments before being implemented in clinical practice.

#### 5 REFERENCES

- [1] Topoleski, L.D., Ducheyne, P., Cuckler, J.M., A fractographic analysis of in vivo poly(methyl methacrylate) bone cement failure mechanisms, *J Biomed Mater Res*, 24, 135-154, 1990
- [2] de Wijn, J.R., Slooff, T.J., Driessens, F.C., Characterization of bone cements, *Acta Orthop Scand*, 46, 38-51, 1975
- [3] Beaumont, P.W., Fracture processes in acrylic bone cement containing barium sulphate dispersions, *J Biomed Eng*, 1, 147-152, 1979
- [4] Demian, H.W., McDermott, K., Regulatory perspective on characterization and testing of orthopedic bone cement, *Biomaterials*, 19, 1607-1618, 1998
- [5] Topoleski, L.D., Ducheyne, P.m Cuckler, J.M., Microstructural pathway of fracture in poly(methyl methacrylate) bone cement, *Biomaterials*, 14, 1165-1172, 1993

#### 6 ACKNOWLEDGMENTS

This study received financial support from the Brigham Orthopaedic Foundation. We thank Dr. David Baker and Professor Lisa Pruitt of the University of California at Berkeley for performing fatigue experiments, and Dr. Peter Jemian and Dr. Jan Ilavsky of the National Institute of Standards and Technology for their assistance with USAXS measurements. The UNI-CAT facility at the Advanced Photon Source (APS) is supported by the University of Illinois at Urbana Champaign, Materials Research Laboratory (U.S. Department of Energy, the State of Illinois-IBHE-HECA, and the National Science Foundation), the Oak Ridge National Laboratory (U.S. Department of Energy), the National Institute of Standards and Technology (U.S. Department of Commerce), and UOP LLC. The APS is supported by the U.S. Department of Energy, Office of Science, Office of Basic Energy Sciences, under Contract No. W-31-109-ENG-38.